Performance Assessment of Heat Pump and Solar Thermal Heating with Seasonal Storage Systems for Smart Microgrid Research Center Building at IAUN

S.M.Hasan Zanjani
Faculty of Architecture & Urbanism
Tabriz Islamic Art University
Tabriz, Iran
mh.zanjani@tabriziau.ac.ir

Hossein Shahinzadeh
Department of Electrical Engineering
Amirkabir University of Technology
Tehran, Iran
h.s.shahinzadeh@ieee.org

Azita Balali Oskui
Faculty of Architecture & Urbanism
Tabriz Islamic Art University
Tabriz, Iran
a.oskoyi@tabriziau.ac.ir

Wahiba Yaïci
CanmetENERGY Research Centre
Natural Resources Canada
Ottawa, Canada
wahiba.yaici@nrcan-rncan.gc.ca

Michela Longo
Department of Energy
Politecnico di Milano
Milan, Italy
michela.longo@polimi.it

S. Mohammadali Zanjani*
Smart Microgrid Research Center,
Najafabad Branch, Islamic Azad University,
Najafabad, Iran
sma_zanjani@pel.iaun.ac.ir

***Abstract*— In this research, the building of the Intelligent Microgrid Research Center in Islamic Azad University, Najafabad Branch (IAUN), has been selected as a sample space. The energy required to heat the building is transferred to the seasonal storage tank in the basement by flat solar collectors with an installation angle of 47.5°. This heat is transferred to the internal space via a geothermal heat pump in the winter. The thermodynamic study of the proposed system is simulated by MATLAB software. The system losses have also been evaluated, and thereby an optimal solar heating system procures all heat demand of the building. The required collector surface is 240 square meters, the tank volume is 2200 cubic meters, and the insulation thickness is 1.2 meters.**

Keywords— Flat Solar Collector, Seasonal Storage Tank, Building Heating, Geothermal Heat Pump, Solar Radiation, Energy Management

I. INTRODUCTION

One of the main needs of human beings today is to achieve comfort in their living environment. However, the optimal temperature of the living space is one of the most important factors in achieving these comfort conditions [1]. Due to the growing human need for thermal comfort, today, various heating supply systems are on the market to solve, each of which has a different amount of energy consumption [2]. One of the types of systems is flat solar collectors as well as geothermal heat pumps. In this research, we will examine the use of a combination of these two systems with a seasonal heat storage tank. The reason for using renewable energy is that fossil fuels are finite and cause air pollution and an imbalance of supply and demand [3-5]. The study space in this research is the Intelligent Microgrid Research Center building at IAUN, with a default area of 825 square meters and a ceiling height of 3 meters in the city of Najafabad, which uses a geothermal heat pump system for heating. In order to increase the efficiency of the heat pump, a seasonal solar-powered energy storage facility is employed [6]. By utilizing a flat solar collector, the tank temperature and consequently heat pump efficiency are increased, and the level of power consumption is mitigated. [7-8].

II. SOLAR COLLECTOR

A solar collector is a special heat exchanger that converts solar radiation energy into heat. Solar collectors differ from conventional heat exchangers in several ways. Heat exchangers usually carry out liquid-to-liquid heat exchange, which occurs at a high heat transfer rate and ignores the radiation [9]. In a solar collector, radiant energy is received by the absorber plate from the sun at a great distance and is transferred to the fluid as thermal energy [10]. The intensity of the impact radiation is, at best, approximately 1100 watts per square meter (without an optical concentrator) and is variable. The wavelength range is from 0.3 to 3μm, which is significantly smaller than the radiation emitted from many energies absorbing surfaces, which have more energy according to Equation (1).

$$E = nh\frac{C}{\lambda} \tag{1}$$

Flat collectors have the ability to increase the temperature of the inlet fluid up to 100° C above the environment temperature. These collectors absorb both direct and scattered solar radiation and do not require sun tracking and do not require special maintenance, and are also mechanically simpler than concentrating collectors [11].

A. Average monthly absorbed radiation

Klein obtained the absorbed solar radiation on average monthly in this way and used a lot of data. He stated that the product of the multiplication coefficients of the monthly average absorption gives us the monthly average absorbed radiation ($\overline{S}$) when multiplied by the impact of the monthly average on the collector. Equation (1) gives the absorbed average monthly radiation using the uniform scatter in all directions [12]:

$$\overline{S} = \begin{cases} \overline{H}_B \overline{R}_b \left(\overline{\tau\alpha}\right)_b + \overline{H}_D \left(\overline{\tau\alpha}\right)_d \left((1+\cos\beta)/2\right) \\ +\overline{H}\rho_g \left(\overline{\tau\alpha}\right)_g \left((1-\cos\beta)/2\right) \end{cases} \tag{2}$$

The parameters of scattered absorption-scattering coefficient and reflected from the ground ($\left(\overline{\tau\alpha}\right)_d$ & $\left(\overline{\tau\alpha}\right)_g$) can be evaluated using the effective impact angle shown in Figure (1). For calculating the direct monthly average radiation, Klein introduced a function according to the collector slope, moon, latitude, and collector side angle. The angle of direct collision (equivalent) to the monthly average is obtained. The diagram of this function is shown in Figure (2) [13]. The $\overline{\theta}_b$ values obtained are evaluated using Figure

* Assistant Professor, Department of Electrical Engineering, Najafabad Branch, Islamic Azad University, Najafabad, Iran.

(3), shown in the angle distribution. From Figure (1), for the collector with an installation angle of 47.5°, the effective angle of impact of the radiated radiation from the sky is 55 °, and the effective angle of the impact of the reflected radiation from the ground is 67 °. $(\tau\alpha)_n = 0.76$ is obtained from Figure (2) for angles of 55° and 67°. Therefore $\left(\overline{\tau\alpha}\right)_d = 0.68$ and $\left(\overline{\tau\alpha}\right)_g = 0.6$ is considered. These values, as mentioned, apply to all months.

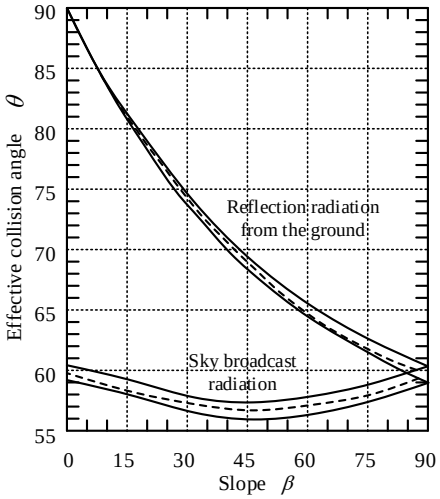

Fig. 1. The angle of collision of uniform scattered radiation and uniform radiation reflected from the ground on sloping surfaces

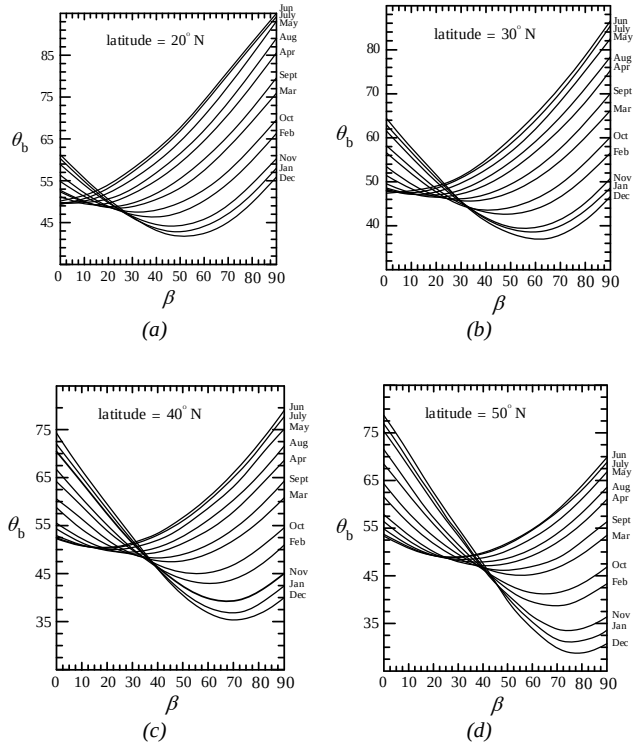

Fig. 2. The angle of direct average monthly radiation for different positions and directions of the collector surface

B. Angle of inclination

The angle of inclination, the position of the angles of the sun at noon (when the sun is at its local peak), can be calculated from the approximate equation "Cooper" by considering the positive $-23.45° \le \delta \le 23.45°$ of the surface, north, and equator [14]:

$$\delta = 23.45 \times \sin\left(360\left((284+n)/365\right)\right) \quad (3)$$

In the above equation, "n" represents the day of the year.

C. Sunset angle

The angle of the sunset is denoted by ω_s which $\theta_z = 90°$ (for horizontal surfaces, the angle of incidence is equal to the angle of the apex of the sun) is obtained from the following equation [15]:

$$\omega_s = \cos^{-1}\left[-\tan\phi\tan\delta\right] \quad (4)$$

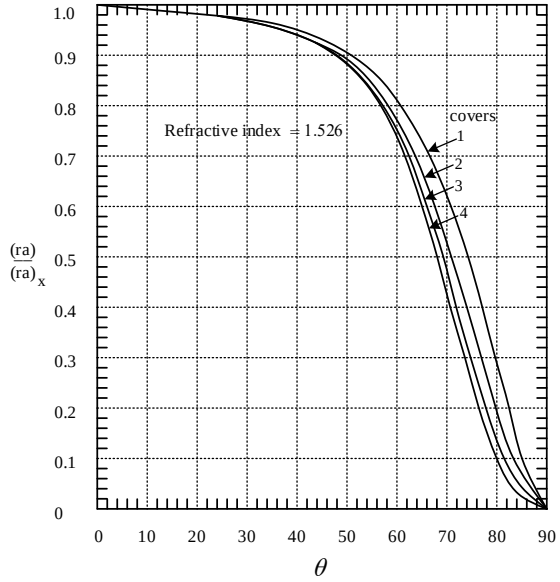

Fig. 3. $(\tau\alpha)/(\tau\alpha)_n$ Common curves for one to four coatings

D. Broadcast components and direct monthly radiation

The average monthly filtration index $\overline{K}_T$ is the ratio of the average monthly average of daily radiation on a horizontal surface to the monthly average of daily external radiation, which is obtained from the following equation [16]:

$$\overline{K}_T = \overline{H}/\overline{H}_0 \quad (5)$$

To determine the monthly average of daily scattered radiation on a horizontal surface with respect to the angle of the sun and the index of clear sky, we use the following equations [17]:

$$\begin{cases} \dfrac{\overline{H}_D}{\overline{H}} = 1.391 - 3.56\overline{K}_T + 4.189\overline{K}_T^2 - 2.137\overline{K}_T^3 \\ \omega_s < 81.4^o, 0.3 \le \overline{K}_T \le 0.8 \end{cases} \quad (6)$$

$$\begin{cases} \dfrac{\overline{H}_D}{\overline{H}} = 1.311 - 3.022\overline{K}_T + 3.427\overline{K}_T^2 - 1.821\overline{K}_T^3 \\ \omega_s < 81.4^o, 0.3 \le \overline{K}_T \le 0.8 \end{cases} \quad (7)$$

The value of $\overline{H}_B$ will also be obtained by determining the value of $\overline{H}_D$ from the following equation [18]:

$$\overline{H}_B = \overline{H} - \overline{H}_D \quad (8)$$

The geometric factor for direct radiation is $\overline{R}_b$. $\overline{R}_b$ is the ratio of the average daily direct radiation on a sloping surface to the average daily direct radiation on a horizontal surface for the target moon is as follows for sloping surfaces facing the equator in the Northern Hemisphere [19]:

$$\overline{R}_b = \frac{\cos(\phi-\beta)\cos\delta\sin\omega_s + (\pi/180)\omega_s'\sin(\phi-\beta)\sin\delta}{\cos\phi\cos\delta\sin\omega_s + (\pi/180)\omega_s\sin\phi\sin\delta} \quad (9)$$

ω_s' And the angle of sunset for the slope for the average day of the month is obtained from the following relation:

$$\omega_s' = Min\begin{bmatrix} \cos^{-1}\left(-\tan\phi\tan\delta\right) \\ \cos^{-1}\left(-\tan\left(\phi-\beta\right)\tan\delta\right) \end{bmatrix} \quad (10)$$

The fraction form in Equation (10) is the extrinsic radiation on the sloping surface, and its denominator is the extrinsic radiation on the horizontal surface [20].

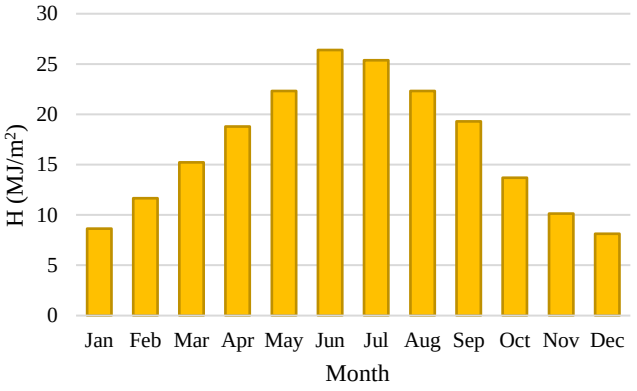

Fig. 4. The monthly amount of daily radiation received from the horizon for the city of Najafabad

E. *Heat lost in the collector*

Before determining the effective heat captured by the collector, it is essential to calculate the heat wasted from the collector surface, which can be found in the following parts. The absorption coefficient of the collector is 0.76, and two general coefficients associated with collector heat loss are both considered by 4.6 W/m^2-$C°$, with a glass cover [21]. The following equation yields the intensity of mean heat loss dissipated from the surface of the collector in monthly intervals [22]:

$$Q_{Loss} = U_L\left(T_i - T_\alpha\right) \quad (11)$$

The cold season in Najafabad usually starts in December, and the highest temperature of the year is observed in August. According to the 10-year meteorological statistics (2010-2020) at Najafabad meteorological station, we will need heating for Najafabad city from early November to late April and cooling from early June to early October. Figure (5) shows the average temperature of Najafabad in the 10 years under study [23].

F. *Useful energy received by the collector*

When the entire collector is at the temperature of the inlet fluid, the possible useful energy received (heat transfer) in a solar collector reaches its maximum value. In this case, heat loss to the environment is minimized. The actual effective energy gained by the collector is the summation of a mathematical term, which multiplies the collector heat dissipation (heat loss) factor by the highest feasible harvestable energy absorbed, which is given in Equation (12). The heat dissipation factor is considered to be 0.95.

$$Q_U - A_C F_R\left[\overline{S} - U_L\left(T_i - T_\alpha\right)\right] \quad (12)$$

It is crucial to estimate the entering fluid average temperature into the collector, as well as the maximum temperature inside and around the reservoir tank, in order to find the minimum and maximum level of useful heat that can be extracted harvested from the collector. According to previous examples, different patterns can be used for this purpose.

a) Maximum temperature 82° C [24]

b) Increasing the tank temperature by 50° C [25]

c) Maximum temperature 70° C

d) Maximum temperature 75° C

The maximum temperature level of 69° C inside the tank yields the maximum level of usable energy being captured by the collector. As a result, for the purposes of reservoir design (Tank in the depth of soil), a maximum temperature limit of 69° C is taken into account.

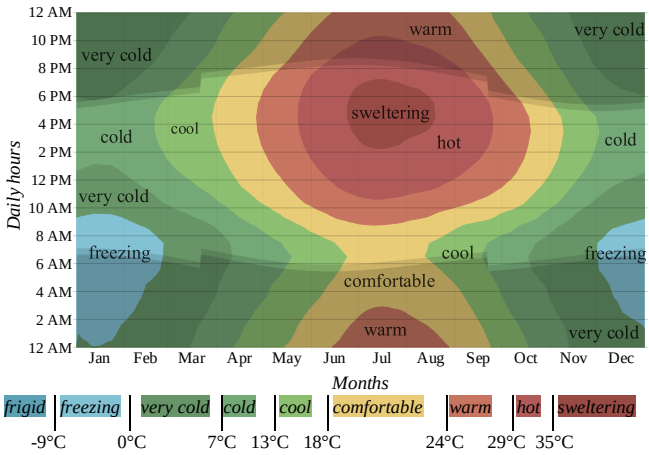

Fig. 5. The average temperature of Najafabad in the 10 years studied (2010–2020)

III. HEAT TRANSFER IN THE BUILDING

Calculate the conduction heat transmitted by the building walls such as walls, ceilings, floors, doors, windows, and glass from the following formula:

$$Q = AU\left(t_1 - t_2\right) \quad (13)$$

Air infiltration into the building is always one of the most important ways to dissipate heat (in winter) and absorb heat in summer [26]. The following formula is used to calculate the amount of infiltrating air:

$$V = v \times n \quad (14)$$

As can be deduced from equation (14), in this method, the amount of infiltrating air is satisfied based on the number of times the room air is exchanged with fresh air in one hour.

TABLE I. NUMBER OF ROOM AIR CHANGES PER HOUR [27]

Frequency of air change per hour (n)	Room Type
1	For rooms with a wall, door and window facing outside.
1.5	For rooms with two walls, door and window facing outside.
2	For rooms with doors and windows from three or four walls.
2	For the hallways of the entrance of the building
0.5	For rooms or spaces lacking doors and windows facing the outside, such as the hall or hall, which are located in the middle of the building.

After calculating the volume of infiltrating air into the room, we calculate the amount of heat load through the following formula [28]:

$$Q = V \times 0.0749 \times 0.241 \times \left(t_i - t_o\right) \quad (15)$$

The Smart Microgrid Research Center building with an area of 825m^2 and a ceiling height of 3m is assumed. This building is located in IAUN, Najafabad city, which is shown in Figure (6), the location of the spaces, and the facade images of the building.

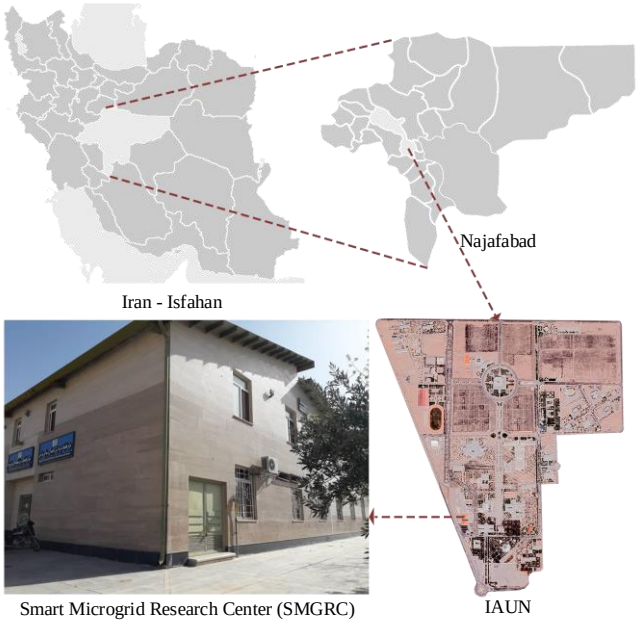

Fig. 6. Location of spaces and facade images of the building understudy

Stone surface with a thickness of 2cm, hollow brick with a thickness of 10cm, and internal joinery of Ceramic Tiles (thickness of 2cm) have been used in the construction of the walls of the building. This building has double-leaf glass doors with a 4.2 m^2 Area and 29 glass windows with a 52.2 m^2 Area, which has 1.2 $W/m^2\text{-}C^\circ$ heat transfer coefficient [29]. As shown in Figure (7), the required heat load for the heat demands of the building during cold weather months is estimated via the maximum and the mean monthly air temperatures in Najafabad as inputs.

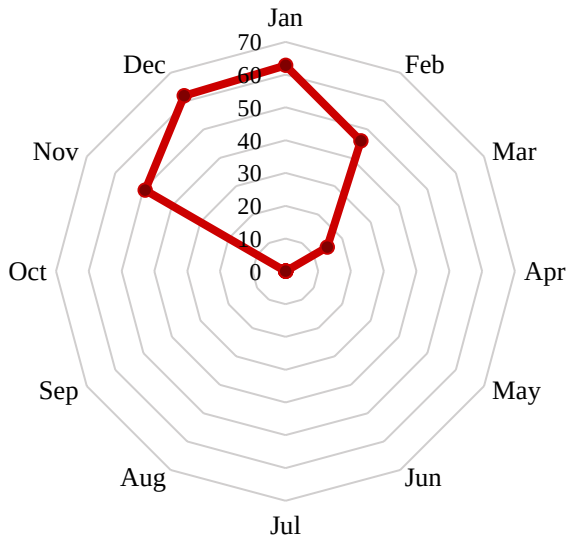

Fig. 7. The heat demand in the building during cold months (kW)

Since this model tries to procure and transmit all demanded energy necessary required to satisfy the heat demands of internal loads in the building by the solar collector, the total area covered by the collector surface must be sufficiently wide to capture enough energy and transport it to the energy reservoir tank, as shown in the illustration. It is necessary to note that not all the stored energy in the tank is retained, and some are lost; hence, the storage tank must be effectively insulated. The insulation is assumed to operate in such a way that 10% of the stored energy is dissipated [30]. The following equation gives the collector level:

$$A_C = Q_h / 0.9 q_U \tag{16}$$

IV. Storage Tank

There is a solar-powered storage tank in a soil-filled basement. Ten barrels of 220 liters of water are put inside of the tank in order to accept heat water fluid from solar collectors and transmit the heat to the soil gradually over time [31]. The following equation is given to calculate the storage tank volume:

$$V = \left(\frac{0.9 \sum_{i=4}^{10} Q_{U_i}}{T_{\max} - T_0} - \rho_w Cp_w V_w \right) / \rho_s Cp_s \tag{17}$$

In Equation (17), the parameter "*i*" is the number of months, which according to the above equation, the volume of soil is 1200 m^2. As mentioned earlier, the basement soil temperature at a depth of 7 meters and above is approximately constant and is equal to 18°C [32]. The tank is placed in the basement at 7.5 meters in depth to maintain the total temperature uniformity around the reservoir.

V. Tank Insulation

A uniform condition and the one-dimensional conductivity are maintained, subject to calculating the insulation thickness employing Fourier law and calculating thermal flow received from the wall of the insulated tank. To insulate the tank, we use mineral wool with 0.0387 $W/m^2\text{-}C^\circ$ amount of thermal conductivity [33]:

$$\begin{cases} H\iota_{st} = 0.1Cap = \dfrac{k_{ins} SA_{st} \Delta T_{st-g}\, 3.156\times10^7 \dfrac{\text{second}}{year} \dfrac{GJ}{10^9 J}}{th_{ins}} \\ Th_{ins} = \dfrac{k_{ins} SA_{st} \Delta T_{st-g}\, 3.156\times10^7 \dfrac{\text{second}}{year} \dfrac{GJ}{10^9 J}}{H\iota_{st}} \end{cases} \tag{18}$$

From the above equation, the insulation thickness will be equal to 1.2m.

VI. Geothermal Heat Pump Model

A device called "Ground Source Heat Pumps (GSHPs) is needed to transfer heat from the basement into the building, or vice versa." To calculate the COP of the heat pump, in the months that the heat pump will be called for in operation for heating, the tank temperature is required. The monthly temperature can be obtained using the energy balance of the tank while assuming that the heat lost in the tank is 10% of the heat stored in the tank.

$$T_2 = \frac{(0.9Q_U - Q_h)10^6 \dfrac{J}{1MJ}}{(\rho_s V_s Cp_s + \rho_w V_w Cp_w)} + T_1 \tag{19}$$

Experience has conveyed that the heat pump performance is almost half of the operational state in the Carno cycle [34]. Regarding the temperature values that were acquired, the coefficient of performance associated with the heat pump that was used in accordance with the ideal cycle is 18.05., and the performance coefficient of the heat pump in the real case will be 9.025. Figure (8) shows the structure of the proposed system.

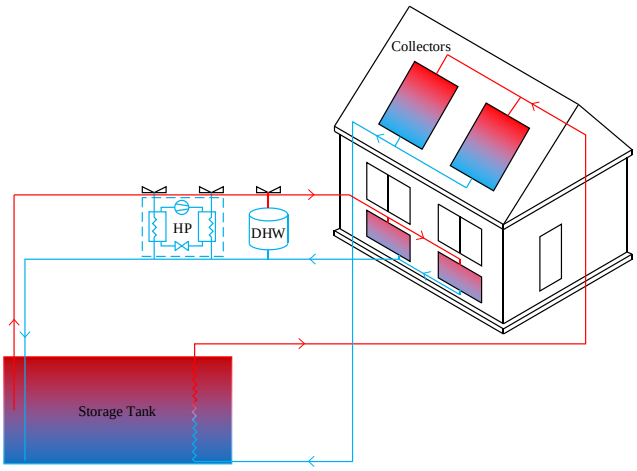

Fig. 8. The structure of the proposed system for heating the building of the Intelligent Microgrid Research Center

VII. Results related to calculations

The results of the calculations will be as follows:

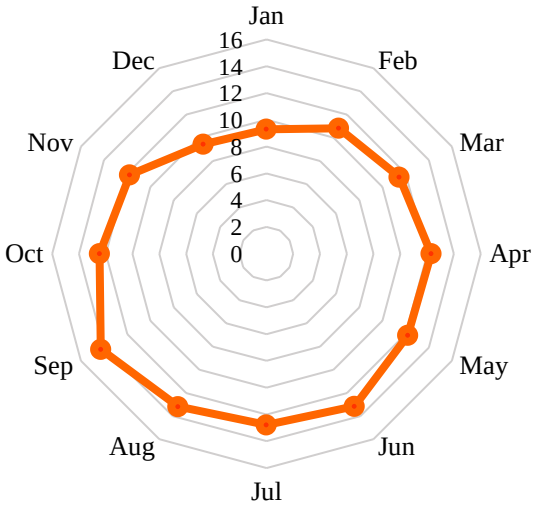

Fig. 9. Mean radiation absorbed by the collector during different months in terms of (MJ/m^2)

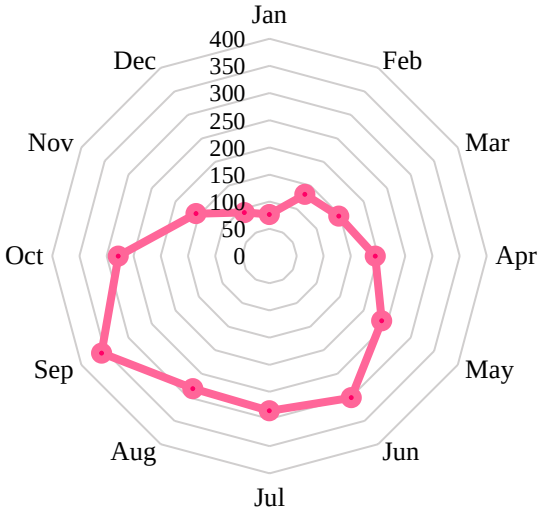

Fig. 10. The monthly useful energy of the collector to increase the tank temperature by 50° C for different months in terms of (MJ/m^2)

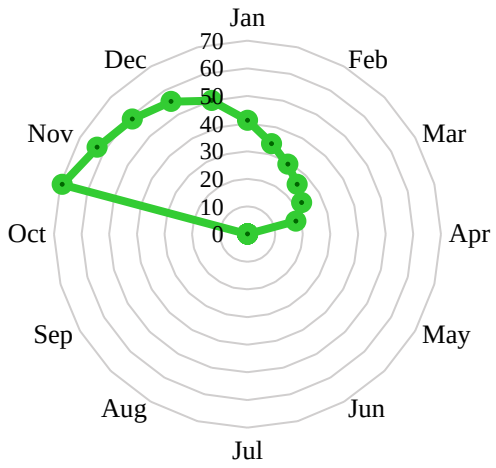

Fig. 11. Storage tank temperature changes in cold months at ° C

VIII. Conclusions and suggestions

The obtained results of this study imply the following conclusions.

1) Due to the fact that the temperature of the soil is almost constant when the tank is placed at a depth of 6-7 m in the basement. That is why the proposed model is an excellent seasonal storage tank. In comparison to water, the advantage of soil is that water might leak outside of the tank or evaporate gradually over time, causing damage to the system and demanding the refilling of wasted water, whereas soil does not have a similar drawback. Understandably, because the soil has a lower specific heat capacity than water, a larger storage tank is needed to incorporate soil-based storage.
2) The useful energy collected by the collector diminishes as the maximum temperature of the storage tank rises, and the capacity of the storage tank decreases as well. An appropriate and sensible balance between the maximum internal tank temperature and the corresponding volume should be considered to take the limitations pertaining to the building dimensions into account.
3) In such a system, the heat is gradually stored for several months in the heat storage, which is why it does not require a large-scale collector cross-section.
4) Solar devices such as linear parabolic collectors and heat pipes are incorporated to considerably boost the tank temperature in big residential buildings, business centers, hospitals, shopping malls, hotels, etc.
5) Due to the fact that the tank temperature exceeds the inside design temperature, the coefficient of performance (COP) associated with the heat pump will play a substantial role. In fact, the higher the tank temperature, the greater is the coefficient of performance of the pump.
6) Generated Energy from a photovoltaic system is to supply power to the heat pump.
7) The efficiency of collectors can be determined by the maximum permitted temperature of the tank, the absorber's material, and the collector installation slope, as well as some other implementing indicators. The case Najafabad University has a maximum temperature of approximately 34°.

8) It is highly recommended to utilize a small-scale auxiliary heating system in parallel with this system, which can be called in case of failures, emergencies, or unwanted crises.
9) Using the heat pump system in the cooling season and transferring its heat to the storage tank.

REFERENCES

[1] Mehmood, U., Agyekum, E. B., Kamel, S., Shahinzadeh, H., & Moshayedi, A. J. (2022). Exploring the Roles of Renewable Energy, Education Spending, and CO2 Emissions towards Health Spending in South Asian Countries. *Sustainability*, *14*(6), 3549.

[2] Nematollahi, A. F., Shahinzadeh, H., Nafisi, H., Vahidi, B., Amirat, Y., & Benbouzid, M. (2021). Sizing and Sitting of DERs in Active Distribution Networks Incorporating Load Prevailing Uncertainties Using Probabilistic Approaches. *Applied Sciences*, *11*(9), 4156.

[3] Diwania, S., Agrawal, S., Siddiqui, A. S., & Singh, S. (2020). Photovoltaic–thermal (PV/T) technology: a comprehensive review on applications and its advancement. *International Journal of Energy and Environmental Engineering*, *11*(1), 33-54.

[4] Huang, H., Xiao, Y., Lin, J., Zhou, T., Liu, Y., & Zhao, Q. (2020). Thermal characteristics of a seasonal solar assisted heat pump heating system with an underground tank. *Sustainable Cities and Society*, *53*, 101910.

[5] Kalantar, V., & Khayyaminejad, A. (2022). Numerical simulation of a combination of a new solar ventilator and geothermal heat exchanger for natural ventilation and space cooling. *International Journal of Energy and Environmental Engineering*, 1-20.

[6] Ismaeel, H. H., & Yumrutaş, R. (2020). Investigation of a solar assisted heat pump wheat drying system with underground thermal energy storage tank. *Solar Energy*, *199*, 538-551.

[7] Pinamonti, M., Beausoleil-Morrison, I., Prada, A., & Baggio, P. (2021). Water-to-water heat pump integration in a solar seasonal storage system for space heating and domestic hot water production of a single-family house in a cold climate. *Solar Energy*, *213*, 300-311.

[8] Lu, J., He, G., & Mao, F. (2020). Solar seasonal thermal energy storage for space heating in residential buildings: Optimization and comparison with an air-source heat pump. *Energy Sources, Part B: Economics, Planning, and Policy*, *15*(5), 279-296.

[9] Gül, Ö., & Ülker, T. (2020, October). Economic evaluation of dynamic thermal rating under variable loading conditions for the flexibility of power systems with wind power plants. In *2020 2nd Global Power, Energy and Communication Conference (GPECOM)* (pp. 214-219). IEEE.

[10] Kim, T., Choi, B. I., Han, Y. S., & Do, K. H. (2018). A comparative investigation of solar-assisted heat pumps with solar thermal collectors for a hot water supply system. *Energy Conversion and Management*, *172*, 472-484.

[11] Beausoleil-Morrison, I., Kemery, B., Wills, A. D., & Meister, C. (2019). Design and simulated performance of a solar-thermal system employing seasonal storage for providing the majority of space heating and domestic hot water heating needs to a single-family house in a cold climate. *Solar Energy*, *191*, 57-69.

[12] Abujubbeh, M., & Fahrioglu, M. (2019, June). Determining maximum allowable pv penetration level in transmission networks: Case analysis-northern cyprus power system. In *2019 1st Global Power, Energy and Communication Conference (GPECOM)* (pp. 292-297). IEEE.

[13] Wole-Osho, Ifeoluwa, Eric C. Okonkwo, Serkan Abbasoglu, and Doga Kavaz. "Nanofluids in solar thermal collectors: review and limitations." *International Journal of Thermophysics* 41, no. 11 (2020): 1-74.

[14] Taamneh, Y., Manokar, A. M., Thalib, M. M., Kabeel, A. E., Sathyamurthy, R., & Chamkha, A. J. (2020). Extraction of drinking water from modified inclined solar still incorporated with spiral tube solar water heater. *Journal of Water Process Engineering*, *38*, 101613.

[15] Sing, C. K. L., Lim, J. S., Walmsley, T. G., Liew, P. Y., Goto, M., & Bin Shaikh Salim, S. A. Z. (2020). Time-dependent integration of solar thermal technology in industrial processes. *Sustainability*, *12*(6), 2322.

[16] Kabiri, S., Manesh, M. K., Yazdi, M., & Amidpour, M. (2020). Dynamic and economical procedure for solar parallel feedwater heating repowering of steam power plants. *Applied Thermal Engineering*, *181*, 115970.

[17] Tregambi, C., Bareschino, P., Mancusi, E., Pepe, F., Montagnaro, F., Solimene, R., & Salatino, P. (2021). Modelling of a concentrated solar power–photovoltaics hybrid plant for carbon dioxide capture and utilization via calcium looping and methanation. *Energy Conversion and Management*, *230*, 113792.

[18] Li, C., Li, C., Lyu, Y., & Qiu, Z. (2020, June). Performance of double-circulation water-flow window system as solar collector and indoor heating terminal. In *Building Simulation* (Vol. 13, No. 3, pp. 575-584). Tsinghua University Press.

[19] Aykut, E., & Terzi, Ü. K. (2020). Techno-economic and environmental analysis of grid connected hybrid wind/photovoltaic/biomass system for Marmara University Goztepe campus. *International Journal of Green Energy*, *17*(15), 1036-1043.

[20] Tahir, S., Ahmad, M., Abd-ur-Rehman, H. M., & Shakir, S. (2021). Techno-economic assessment of concentrated solar thermal power generation and potential barriers in its deployment in Pakistan. *Journal of Cleaner Production*, *293*, 126125.

[21] Pourfayaz, F., Shirmohammadi, R., Maleki, A., & Kasaeian, A. (2020). Improvement of solar flat-plate collector performance by optimum tilt angle and minimizing top heat loss coefficient using particle swarm optimization. *Energy Science & Engineering*, *8*(8), 2771-2783.

[22] Zhu, Y., Li, P., Ruan, Z., & Yuan, Y. (2022). A model and thermal loss evaluation of a direct-absorption solar collector under the influence of radiation. *Energy Conversion and Management*, *251*, 114933.

[23] Mirhedayati, A. S., Hadadi, Z., Zanjani, S. M., Shahinzadeh, H., Bayindir, R., Shaneh, M., & Moradi, J. (2021). Optimal operation of combined heat and power in competitive electricity markets: a case study in IAUN. *International Journal of Renewable Energy Research (IJRER)*, *11*(3), 1013-1022.

[24] Kılıçkap, S., El, E., & Yıldız, C. (2018). Investigation of the effect on the efficiency of phase change material placed in solar collector tank. *Thermal Science and Engineering Progress*, *5*, 25-31.

[25] Moravej, M., Saffarian, M. R., Li, L. K., Doranehgard, M. H., & Xiong, Q. (2020). Experimental investigation of circular flat-panel collector performance with spiral pipes. *Journal of Thermal Analysis and Calorimetry*, *140*(3), 1229-1236.

[26] Hu, Z. X., Cui, G. X., & Zhang, Z. S. (2018). Numerical study of mixed convective heat transfer coefficients for building cluster. *Journal of Wind Engineering and Industrial Aerodynamics*, *172*, 170-180.

[27] Rosti, B., Omidvar, A., & Monghasemi, N. (2019). Optimum position and distribution of insulation layers for exterior walls of a building conditioned by earth-air heat exchanger. *Applied Thermal Engineering*, *163*, 114362.

[28] Ren, C., & Cao, S. J. (2019). Development and application of linear ventilation and temperature models for indoor environmental prediction and HVAC systems control. *Sustainable Cities and Society*, *51*, 101673.

[29] Khan, R. J., Bhuiyan, M. Z. H., & Ahmed, D. H. (2020). Investigation of heat transfer of a building wall in the presence of phase change material (PCM). *Energy and Built Environment*, *1*(2), 199-206.

[30] Yu, J., Kang, Y., & Zhai, Z. J. (2020). Comparison of ground coupled heat transfer models for predicting underground building energy consumption. *Journal of Building Engineering*, *32*, 101808.

[31] Dahash, A., Ochs, F., Janetti, M. B., & Streicher, W. (2019). Advances in seasonal thermal energy storage for solar district heating applications: A critical review on large-scale hot-water tank and pit thermal energy storage systems. *Applied Energy*, *239*, 296-315.

[32] Del Amo, A., Martínez-Gracia, A., Pintanel, T., Bayod-Rújula, A. A., & Torné, S. (2020). Analysis and optimization of a heat pump system coupled to an installation of PVT panels and a seasonal storage tank on an educational building. *Energy and Buildings*, *226*, 110373.

[33] Naranjo-Mendoza, C., Oyinlola, M. A., Wright, A. J., & Greenough, R. M. (2019). Experimental study of a domestic solar-assisted ground source heat pump with seasonal underground thermal energy storage through shallow boreholes. *Applied Thermal Engineering*, *162*, 114218.

[34] Yang, W., Zhang, H., & Liang, X. (2018). Experimental performance evaluation and parametric study of a solar-ground source heat pump system operated in heating modes. *Energy*, *149*, 173-189.